



A Molecular Dynamics and Quantum Mechanics Modeling of Single Crystal Silicon Nanowire Structures

Kausala Mylvaganam and Liangchi Zhang*

School of Aerospace, Mechanical and Mechatronic Engineering, The University of Sydney, NSW 2006, Australia

One-dimensional nanowires play an integral part in the fabrication of nano devices and interconnect. This paper presents the structure, shape and band gap of one-dimensional single crystal silicon nanowires using the molecular dynamics and quantum mechanics methods. Silicon nanowire models of octagonal, circular, hexagonal, rhombohedral, square, and triangular cross-sections along $\langle 110 \rangle$ direction with diameters between 1 and 3 nm were investigated. It was found that for a given shape the energy per atom and the strain energy decrease as the diameter increases, indicating that wires of larger diameters are more stable. Octagonal, circular and hexagonal shapes have lower strain energies due to the higher atomic density of atoms on the surface and therefore more stable. The Density Functional Theory (DFT) calculations showed that the electronic band-gap increases as the diameter decreases. This opens the possibility for light emitting diodes. The SiH_2 phase formed on the $\langle 001 \rangle$ facet of the hexagonal nanowire has a single domain Si—H bonds.

Keywords: Silicon Nanowire, Molecular Dynamics, DFT, Tersoff Potential, Structure, Bandgap.

1. INTRODUCTION

One dimensional nano materials in the forms of tubes, wires and belts have been used as building blocks in the fabrication of nanoelectronic and nanophotonic devices and interconnects. As such there has been a lot of interest in the growth of molecular-scale nanowires and nanotubes. Due to the key role of silicon in the semiconductor industry, silicon nanowires had drawn much attraction. Various technologies have been developed for the fabrication of silicon nanowire, yielding wires of different diameters and orientations. In the past, the silicon nanowires produced were with different orientations and covered with an oxide layer.

Recently Ma et al.¹ and Wu et al.² have fabricated oxide free hydrogen terminated single crystalline silicon nanowires of very small diameters of 1 nm to 7 nm. Ma et al. atomically resolved them using scanning tunneling microscopy (STM) and found that they are more stable than similarly treated silicon wafer surfaces. Most of their STM imaged silicon nanowires had axis along the $\langle 112 \rangle$ direction with a few along the $\langle 110 \rangle$ direction. They also performed scanning tunneling spectroscopy (STS)

measurements and found that the electronic band gap increases from 1.1 to 3.5 eV as the wire diameter decreases from 7 nm to 1.3 nm. This demonstrated the quantum size effect in silicon nanowires which are the basis of the beneficial properties of nanomaterials. For example, the increase in bandgap with decrease in diameter leads to a shift in optical emission from the IR to visible-UV region and opens the possibility for light emitting diodes and lasers. Wu et al.² analyzed the growth axes as a function of diameter using high resolution transmission electron microscopy (HRTEM) and found that 95% of the small diameter (3 nm–10 nm) wires grew along $\langle 110 \rangle$ direction, 61% of the medium diameter (10 nm–20 nm) silicon nanowires grew along $\langle 112 \rangle$ direction and 64% of the large diameter (20 nm–30 nm) wires grew along $\langle 111 \rangle$ direction. On the other hand Barnard et al.³ showed from their theoretical calculations that carbon nanowires with the principal axis in the $\langle 110 \rangle$ direction is less structurally favourable. However, in their studies the diameters of the wires considered were less than 1 nm.

In this work we examine the structure, shape and band gap of one dimensional single crystal silicon nanowire of diameters between 1 nm and 3 nm, generated along $\langle 110 \rangle$ direction using molecular dynamics and quantum mechanics methods.

*Author to whom correspondence should be addressed.

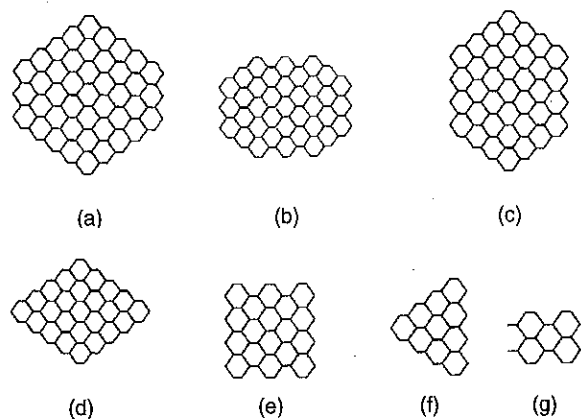


Fig. 1. Cross-sectional shapes of silicon nanowires examined in this work: (a) circular, (b) octagonal, (c) hexagonal, (d) rhombohedral, (e) square, (f) triangular, and (g) rectangular (analogue of the cubic diamond wire in Ref. [3]).

2. COMPUTATIONAL TECHNIQUE

Silicon nanowire models of octagonal, circular, hexagonal, rhombohedral, square, triangular, and rectangular cross-sectional shapes as shown in Figures 1(a)–1(g) with different diameters but all having a length of 301 Å were generated and examined using the classical molecular-dynamics (MD) and quantum mechanics methods. In the MD method the inter-atomic interactions were described by a three-body Tersoff potential,^{4,5} which has been successfully used to simulate various deformation processes of silicon. As pointed out in our earlier work⁶ on nanotubes, in order to minimize the heat conduction problem and improve the computational efficiency, Berendsen thermostat was applied to all atoms except those rigidly held. Their energies were minimized by conjugate gradient method.

A small section of these nanowires were hydrogenated to complete the valence of the dangling Si atoms and the band gaps were calculated using the Density Functional Theory (DFT) with a hybrid functional B3LYP^{7–10} and a 3-21G basis set.¹¹ The hexagonal nanowire structure with a vertical diameter d_v of 15.4 Å and a horizontal diameter d_h of 9.7 Å was hydrogenated and the geometry was optimized at the DFT level.

The present level of calculation, DFT(UB3LYP)/3-21G, is known to produce reasonable results¹² for bond lengths, bond angles and bond energies for a wide range of molecules. The DFT calculations were carried out on a super computer using the *ab-initio* quantum chemistry package, Gaussian03.¹³

3. RESULTS AND DISCUSSION

Various cross sectional shapes of the wires examined are shown in Figures 1(a)–1(g). It should be noted that the cross-sections in Figures 1(a) and 1(e) are not exactly of

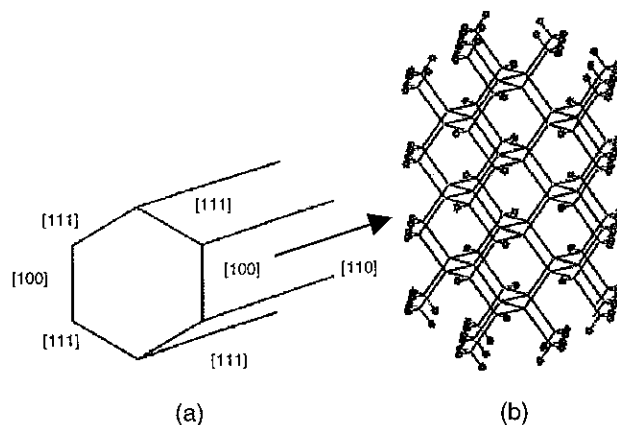


Fig. 2. (a) Schematic three dimensional view of the hexagonal shaped nanowire showing the two [100] surfaces, four [111] surfaces and the axis along [110] and (b) the cross sectional view of the hydrogenated nanowire section used in the DFT study.

circular and square but their vertical and horizontal diameters are nearly equal and their shapes closely resemble a circle and a square respectively. The wire with cross-sectional shape shown in Figure 1(g) is chosen to compare its structure with its carbon analogue³ (i.e., Fig. 2 of Barnard et al.) On minimizing the energy, the shapes of the nanowires did not change significantly; diamond like structure was preserved. The minimum energies, strain energies and the band gap of the nanowires examined are listed in Table I together with their shapes and diameters.

Interestingly, *ab-initio* modeling studies of Barnard et al.³ showed that on relaxation, the cubic diamond nanowire having a diameter of 0.45 nm was transformed into a tube and those having little larger diameter showed some surface reconstruction but preserved the diamond like structure. In that work they have performed Density Functional Theory (DFT) calculations using gradient corrected Vanderbilt type pseudopotentials. So we have repeated the calculations on the cubic diamond nanowire using Tersoff and Tersoff-Brenner potentials to see whether the results of Barnard et al. are potential dependent. For the small diameter ($d_v = 0.38$ nm and $d_h = 0.54$ nm) diamond wire, the calculations with Tersoff-Brenner potential also showed transformation into a tube like structure. The wire with diameter $d_v = 0.5$ nm and $d_h = 0.71$ nm, showed some surface reconstruction but did not transform into tube. Hence the results are not very much potential dependent. In addition the silicon nanowires considered in this work are with diameters greater than 1 nm and therefore any effect of potential will be minimal.

The strain energies of the wires are calculated as the difference in the initial energy and the minimum energy. All the energies are tabulated per atom for comparison purposes. It is clear that the energy per atom decreases as the number of atoms increases and that for a given shape, it decreases as the diameter increases. This is because the large diameter nanowires are less strained. This is

Table I. Various properties of nanowires of different shapes having a length of 301 Å.

Shape	Number of atoms	Diameter (Å)		Minimum energy/ atom (eV)	Strain energy/ atom (eV)	Band gap (eV)
		d_v	d_h			
Circular (I)	8690	26.9	25.9	-4.3282	0.0135	4.32
Octagonal	7742	19.2	25.9	-4.2899	0.0122	3.97
Hexagonal (I)	7584	26.9	20.5	-4.2826	0.0132	3.82
Rhombohedral	5530	19.2	25.9	-4.2820	0.0191	4.18
Circular (II)	5056	19.2	20.8	-4.2449	0.0172	4.06
Triangular (I)	4819	25.9	11.5	-4.1581	0.0193	4.66
Hexagonal (II)	4266	19.2	15.1	-4.1695	0.0158	4.21
Square	4253	15.4	15.1	-4.0668	0.0142	4.29
Triangular (II)	2607	15.4	10.9	-4.0076	0.0222	4.64
Hexagonal (III)	1896	11.5	9.7	-3.9416	0.0193	5.03
Rectangular	1738	10.86	7.68	-3.8811	0.0233	5.34

clearly demonstrated by the strain energy values given in column 5 of Table I. For example, the hexagonal cross sectional shape wires I, II, and III have strain energies of 0.0132, 0.0172, and 0.0193 eV and their diameter decreases on going from I to III; the circular cross sectional wires have strain energies of 0.0135 and 0.0172 eV and their diameter decreases on going from I to II. The silicon analogue of the rectangular carbon nanowire that is the smallest in diameter has the highest strain energy. Octagonal shaped nanowire that is bound by four (111), two (110) and two (100) surfaces, circular and hexagonal shaped nanowires that are bound by four (111) and two (100) surfaces and square shaped nanowires that are bound by two (110) and two (100) surfaces have lower strain energies; circular and hexagonal become almost equal as the diameter increases. Rhombohedral shaped wire that is bound by four (111) surfaces and triangular shaped wires that are bound by two (111) and one (100) surfaces are highly strained. The above phenomenon is similar to that reported by Zhang et al.¹⁴ on mono crystalline copper nanowires, where the hexagonal specimen having four (111) and two (100) surfaces was identified as the best shape as it can maximize the gross density of atoms on the surfaces and minimize the distortion and shrinkage stress.

Comparison of the different shaped wires that are similar in size shows the wires bound by (111) surfaces are highly strained. For example, the rhombohedral wire having four (111) surfaces has a higher strain energy compared to the square shaped wire that has no (111) surfaces. Although the hexagonal(II) and circular(II) wires, have four (111) surfaces, only 65–75% of surface atoms come from (111) surface compared to ~100% for the rhombohedral wire. Moreover, for the octagonal wire having four (111), two (110) and two (100) surfaces, only 46% of the surface atoms comes from (111) surface compared to ~75% for the circular(I) wire. This is in agreement with the results of Barnard et al.'s work³ on diamond nanowires where they found the presence of the C(111) surfaces in nano diamonds promotes instability.

The hexagonal shaped (110) nanowire (diameters $d_v = 15.4$ Å, and $d_h = 9.7$ Å) section having two Si(100)

surfaces that form dihydride phase on hydrogenation and four Si(111) surfaces that form trihydride phase on hydrogenation are shown in Figures 2(a) and 2(b). The DFT(B3LYP)/3-21G optimized structure of Figure 2(b) is shown in Figure 3. This shows the dihydride phase on the Si(100) surfaces of the nanowire has a single domain as reported by Ma et al.¹ The results also showed the shortest distance between two Si atoms that are not bonded is 3.84 Å and the distance between the two H atoms of the SiH₂ phase is 1.63 Å. It should be noted that when both the Si(100) surfaces of the hexagonal shaped nanowire are separated by even numbers of silicon layers then it has

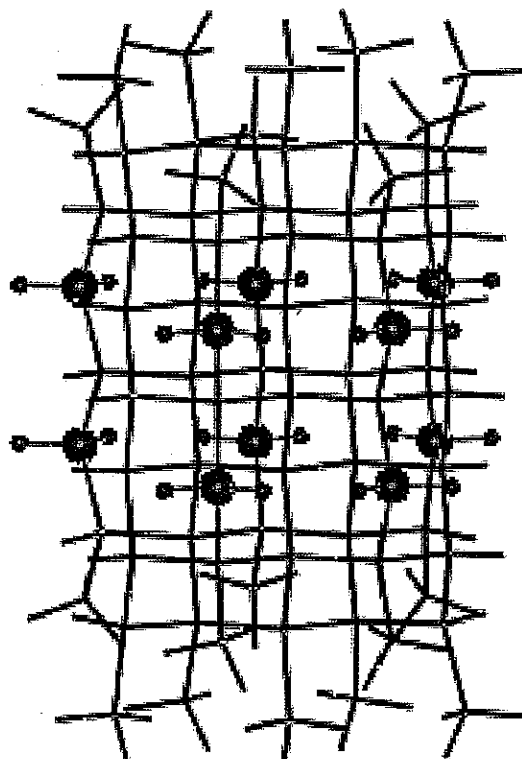


Fig. 3. DFT/3-21G optimized structures of a section of the hexagonal shaped nanowire (hydrogenated) showing SiH₂ single domain on (100) surface.

only one domain which is the case for a regular hexagonal shape. Moreover, according to Ma et al.¹ the SiH₂ phase on the facets of silicon nanowire differs from that found on a flat Si(100) wafer, where two equivalent domains with Si—H bonds orthogonal to each other are found. The geometry of the SiH₂ phase on the nanowire was explained by the existence of a bending stress on the surface of a small diameter wire. We are unable to comment on the geometry of the SiH₂ phase on the Si(100) wafer as quantum mechanical calculations for a larger surface is very expensive.

The band gap is calculated as the difference in energy between the highest occupied molecular orbital (HOMO) and the lowest unoccupied molecular orbital (LUMO). In the above geometry optimization calculations we find that the initial and final (at the optimum geometry) band gap values were nearly the same. As such single point DFT(B3LYP)/3-21G calculations were carried out on small sections of hydrogenated nanowires of all the shapes examined in this study and the HOMO–LUMO difference (i.e., the band gap) is tabulated in the last column of Table I. This shows that for a given shape, the band gap decreases as the diameter increased demonstrating the quantum size effect. For example, among the three hexagonal shaped nanowires studied here, the small diameter wire gave a band gap of 5.03 eV compared to 3.82 eV for the large diameter wire. The above trend is in good accord with the results reported by Ma et al.¹ from their scanning tunneling spectroscopy results.

4. CONCLUSION

Our work demonstrates that (i) for a given shape the energy per atom and the strain energy decrease with the increase in diameter indicating the larger diameter wires are more stable; (ii) octagonal, circular and hexagonal shapes have lower strain energies due to the higher atomic density of atoms on the surface and therefore minimize the distortion and shrinkage stress (iii) the presence of the (111) surface on the nanowire increase the strain energy (iv) the electronic band-gap increases as the diameter decreases which leads to a shift in optical emission from the IR to visible-UV region and opens the possibility

for light emitting diodes and lasers and (v) the SiH₂ phase formed on the (001) facet of the regular hexagonal nanowire has a single domain of Si—H bonds as resolved in the experimental work.

Acknowledgments: The authors thank the Australian Research Council for its continuous financial support. This work was also supported by the Australian partnership for advanced computing.

References

1. D. D. D. Ma, C. S. Lee, F. C. K. Au, S. Y. Tong, and S. T. Lee, *Science* 299, 1874 (2003).
2. Y. Wu, Y. Cui, L. Huynh, C. J. Barrelet, D. C. Bell, and C. M. Lieber, *Nano Lett.* 4, 433 (2004).
3. A. S. Barnard, S. P. Russo, and I. K. Snook, *Nano Lett.* 3, 1323 (2003).
4. J. Tersoff, *Phys. Rev. Lett.* 56, 632 (1986).
5. J. Tersoff, *Phys. Rev. B* 39, 5566 (1989).
6. K. Mylvaganam and L. C. Zhang, *Carbon* 42, 2025 (2004).
7. A. D. Becke, *Phys. Rev. A* 38, 3098 (1988).
8. C. Lee, W. Yang, and R. G. Parr, *Phys. Rev. B* 37, 785 (1988).
9. S. H. Vosko, L. Wilk, and M. Nusair, *Can. J. Phys.* 58, 1200 (1980).
10. A. D. Becke, *J. Chem. Phys.* 98, 5648 (1993).
11. J. S. Binkley, J. A. Pople, and W. J. Hehre, *J. Am. Chem. Soc.* 102, 939 (1980).
12. F. D'Souza, M. E. Zandler, P. M. Smith, G. R. Deviprasad, K. Arkady, M. Fujitsuka, and O. Ito, *J. Phys. Chem. A* 106, 649 (2002).
13. M. J. Frisch, G. W. Trucks, H. B. Schlegel, G. E. Scuseria, M. A. Robb, J. A. M. J. R. Cheeseman, Jr., T. Vreven, K. N. Kudin, J. C. Burant, J. M. Millam, S. S. Iyengar, J. Tomasi, V. Barone, B. Mennucci, M. Cossi, G. Scalmani, N. Rega, G. A. Petersson, H. Nakatsuji, M. Hada, M. Ehara, K. Toyota, R. Fukuda, J. Hasegawa, M. Ishida, T. Nakajima, Y. Honda, O. Kitao, H. Nakai, M. Klene, X. Li, J. E. Knox, H. P. Hratchian, J. B. Cross, C. Adamo, J. Jaramillo, R. Gomperts, R. E. Stratmann, O. Yazyev, A. J. Austin, R. Cammi, C. Pomelli, J. W. Ochterski, P. Y. Ayala, K. Morokuma, G. A. Voth, P. Salvador, J. J. Dannenberg, V. G. Zakrzewski, S. Dapprich, A. D. Daniels, M. C. Strain, O. Farkas, D. K. Malick, A. D. Rabuck, K. Raghavachari, J. B. Foresman, J. V. Ortiz, Q. Cui, A. G. Baboul, S. Clifford, J. Cioslowski, B. B. Stefanov, G. Liu, A. Liashenko, P. Piskorz, I. Komaromi, R. L. Martin, D. J. Fox, T. Keith, M. A. Al-Laham, C. Y. Peng, A. Nanayakkara, M. Challacombe, P. M. W. Gill, B. Johnson, W. Chen, M. W. Wong, C. Gonzalez, and J. A. Pople, *Gaussian 03*, Gaussian, Inc., Wallingford CT, ed. Revision C.02, (2004).
14. L. C. Zhang, H. Tanaka, and P. Gupta, *Key Engineering Materials* 274–276, 331 (2004).

Received: 28 April 2005. Accepted: 9 May 2005.